

WO_x-CeO₂ and WO_x-Nb₂O₅ Catalysts Deactivation During Hexane Isomerization

A.-S. Mamede, E. Payen, and P. Granger

Laboratoire de Catalyse de Lille, UMR CNRS 8010, Université des Sciences et Technologies de Lille, 59 655 Villeneuve d'Ascq, France

M. Florea and V. I. Pârvulescu

Dept. of Chemical Technology and Catalysis, University of Bucharest, B-dul Regina Elisabeta 4-12, Bucharest 030018, Romania

DOI 10.1002/aic.11468

Published online March 17, 2008 in Wiley InterScience (www.interscience.wiley.com).

Two series of WO_x-CeO₂ catalysts containing 10, 12, and 15 wt % W were prepared by co-precipitation and incipient wetness impregnation using a reported procedure. WO_x-Nb₂O₅ catalysts with the same amount of W were prepared by co-precipitation starting from an aqueous solution of ammonium niobium oxalate and ammonium metatungstate with ammonia, until reaching pH 7. After calcining for 3 h in static air at 973 K, the deactivation of the catalysts was investigated using isomerization of hexane as probe reaction at temperatures in the range 393–513 K, both in the absence and in the presence of hydrogen. In-situ Raman spectra during deactivation were recorded as well. The deactivation rate was fitted by an empirical Voorhies equation: $R = m t^{-n}$, where the values of n correlated very well with the mass loss determined from TG analysis. © 2008 American Institute of Chemical Engineers *AIChE J.* 54: 1303–1312, 2008

Keywords: WO_x-CeO₂ and WO_x-Nb₂O₅ catalysts, catalyst deactivation, in-situ Raman investigation, catalysis, degradation

Introduction

Catalysts deactivation by coke deposition is one of the most investigated processes due to the fact that the formation of carbonaceous deposits is an important undesired side reaction in many industrial processes.¹ Coke deposition usually occurs covering the active sites responsible for the reaction, with the associated loss of catalytic activity. If coke build-up rises beyond a certain limit, pore blockage takes place, which removes active sites from contact with the reactant stream at a greater rate than direct site coverage. In extreme cases, interparticle coke growth may increase the pressure drop in fixed bed reactors and ultimately block the passage of fluid.

Several attempts were considered to describe the coke formation. Froment and coworkers provided a quantitative analysis of the deactivation of amorphous catalysts by coke deposition in terms of active site coverage and pore blockage.² In their approach, the catalyst texture is represented by a network of pores structured as a tree, with a degree of branching equal to 2. The bonds of the tree corresponded to the pores of the catalyst, and the nodes to their intersection. To describe the kinetics of the coke deposition these authors used a stochastic model. According to this model two groups of properties seem to control the process. The first group is related to the textural properties of the catalyst, such as the distribution of pore diameters, the catalyst surface area, and the average pore length. The second group relates to the cause of the deactivation, i.e. the formation of coke. It consists of the physical properties of the coke, such as molecular mass and density and of the parameters involved in the rate expressions for coke formation.^{2–5} A much simpler model of

Correspondence concerning this article should be addressed to M. Florea at mihaela.florea@chem.unibuc.ro.

the catalyst deactivation is that described by the empirical Voorhies equation^{1,6}:

$$C = k \cdot t^n \quad (n < 1) \quad (1)$$

Because of its simplicity the Voorhies equation appears to be more versatile and therefore it is still more used in practice.

As mentioned above, the nature of coke is extremely important in describing the catalysts deactivation. Several techniques have been reported to be effective for such a purpose: solvent extraction,⁷ temperature programmed techniques,^{7,8} FTIR,⁷ laser Raman spectroscopy,⁹ ¹³C (CP/MAS) NMR^{10,11}; Pulsed field gradient-nuclear magnetic resonance.¹²

The isomerization of alkanes on acid catalysts is always accompanied by the coke deposition. As for the catalysts, this reaction can be carried out on zeolites,¹³ on supported tungsten oxides¹⁴ or on sulfated zirconia.¹⁵ Under the reaction conditions sulfated zirconia is easily deactivated¹⁶ and to enhance its performances it is necessary to be promoted with Ga¹⁷ or Pt. However, even after promoting, this catalyst is easily deactivated. Keogh et al.¹⁸ considered that the deactivation of Pt-supported on sulfated zirconia catalysts during *n*-hexadecane isomerization is produced by coke deposition on the strong acid sites.

Tungsten supported catalysts are more stable than sulfated zirconia. For these catalysts, Benitez et al. indicated that the nature of coke, olefinic or aromatic, depends on the nature of the support.⁹ When aromatic or pregraphitic coke is generated during reaction, the coke is more difficult to be burnt and produces a higher deactivation.

To have a better view of what is happening during the deactivation and a better control of the deactivation factors it is extremely important to understand the mechanism of the initial coking behavior, since the initial catalyst activity and the extent of the initial deactivation exhibit an important effect on the overall process. Most of the studies consider only the long-term aged catalysts and studies on initial coke formation are scarce.⁷

The addition of hydrogen is improving the isomerization catalyst stability. For sulfated zirconia catalysts, Garin et al.¹⁹ have observed that hydrogen prevents coke formation even in the absence of platinum. The addition of platinum enhances this stability so, it can be concluded that the higher stability observed on Pt-promoted catalysts is due to the presence of both hydrogen and platinum. In the absence of one of them, mainly cracking products and a rapid deactivation were observed.²⁰ For Pt-zeolites it was suggested that protons are formed as charge-compensating cations during reduction by H₂ of metal ions. These protons strongly interact with the reduced transition metal atoms or particles, while they are also bonded to oxide ions of the cage walls. The enhanced stability of these catalysts was associated to the formation of a proton bridge between transition metal and cage as the base of the anchoring phenomena which stabilizes small metal particles.²¹

Experimental

Catalyst preparation

Two series of WO_x-CeO₂ catalysts containing 10, 12, and 15 wt % W were prepared by co-precipitation and incipient

Table 1. Textural Characteristics of the Investigated Catalysts

Catalyst	Preparation Procedure			
	Precipitation		Impregnation	
	W Content, wt %	Surface Area, m ² g ⁻¹	W Content, wt %	Surface Area, m ² g ⁻¹
WO _x -CeO ₂ -10	10	16.3	10	14.5
WO _x -CeO ₂ -12	12	14.0	12	11.8
WO _x -CeO ₂ -15	15	14.0	15	10.8
WO _x -Nb ₂ O ₅ -10	10	22.2	—	—
WO _x -Nb ₂ O ₅ -12	12	18.8	—	—
WO _x -Nb ₂ O ₅ -15	15	16.9	—	—

wetness impregnation using a reported procedure²² WO_x-Nb₂O₅ catalysts with the same amount of W were prepared by co-precipitation starting from an aqueous solution of ammonium niobium oxalate and ammonium metatungstate ((NH₄)₆H₂W₁₂O₄₁·H₂O, Riedel-de Haen) with ammonia, until reaching pH 7. As for WO_x-CeO₂ catalysts, the precipitates were washed, dried, crushed, and calcined for 3 h in static air at 973 K. The catalysts prepared by precipitation would be nominated as P-catalysts, and those prepared by impregnation as I-catalysts.

Catalyst characterization

Chemical analysis of the catalysts was performed by ICP-AES. The W contents are given in Table 1. The BET specific surface areas and the pore size were obtained from nitrogen adsorption isotherms recorded at 77 K with an ASAP 2000 instrument from Micromeritics. The samples were outgassed at 77 K for 12 h under a residual pressure of 0.1 Pa. The surface areas of the catalysts are indicated in the same Table 1.

After the exposure to the catalytic conditions (1, 2, 6, 12, and 48 h), the used catalysts were Soxhlet-extracted with THF, toluene, CH₂Cl₂ and CHCl₃ until no discoloration of the solvent took place anymore. For each extraction about 2 g of used catalyst was placed in a Whatman thimble, which was fitted in the Soxhlet apparatus. During extraction the compartment containing the catalyst was siphoned every 5 min. The extraction temperature was about 338 K. After extraction the sample was dried until its weight did not change anymore. The weights before and after extraction were taken.

Nonactivated samples as well as catalysts exposed to the hydrocarbons were submitted to TG, DTG and HF analyses. The measurements were carried out using a SETARAM 92 16.18 equipment one-line coupled with a quadrupole QMG 311 spectrometer (MS) from Balzers, scanning the masses between 28 and 96. Prior to the analyses, the samples were purged in flowing He at 323 K until the MS signal due to hydrocarbons was no longer detected. The MS was connected to the TG-DTG-HF unit with a teflon tubing kept at 423 K to avoid eventual condensation. The runs were conducted in a stream of helium (99.99% purity, from Belgair). The reactant-loaded samples (typically 75 mg) were heated from ambient temperature to 1073 K at a heating rate of 278 K min⁻¹, with a plateau of 30 min at the final temperature, and then cooled at 323 K. Soon after, the thermal cycle was

repeated, and the data of the second cycle were automatically subtracted from the first cycle data using the apparatus routine program. Both cycles were carried out in flowing helium (200 ml min^{-1}). Platinum pans were used as sample holders, and Al_2O_3 was the reference material. A third cycle was also carried out soon after the samples were again cooled at 323 K in flowing a 10% O_2/He mixture instead of He, with on-line MS analysis of the evolved gases.

NH_3 -DRIFT (diffuse reflectance infrared Fourier transform) spectra were collected with a NICOLET 370 spectrometer (200 scans with a resolution of 4 cm^{-1}). Pure samples were placed inside a commercial controlled environmental chamber attached to a diffuse reflectance accessory (Smart collector). The stability of the adsorbed ammonia species during the increase of temperature was investigated by recording the spectra under flowing helium (30 ml min^{-1}) at room temperature, 373, 473, and 573 K, after exposure to an ammonia flow (30 ml min^{-1}) for 30 min at room temperature.

Catalytic deactivation tests

The catalytic deactivation tests were carried out in a conventional installation, over 50 mg of catalyst powder loaded in a tubular, down-flow-operated quartz microreactor. Hexane was passed through the catalyst bed at a space velocity of $120 \text{ cm}^3 \text{ g}^{-1} \text{ cat h}^{-1}$. Under these conditions the pressure drop was of 2–3 mm H_2O . The reaction was performed at temperatures in the range 393–513 K, both in the absence and in the presence of hydrogen (30 ml min^{-1}). The grain size was approximately. Analysis of the products was achieved in a Varian Star 3400CX gas chromatograph equipped with a Chrompack 7530 capillary column (WCOT fused-silica column with CP-Sil PONA CB stationary phase). The catalytic activity was expressed as transformation rate of hexane and selectivity to dimethylbutane and methylcyclopentane.

In-situ Raman spectra during deactivation were recorded on a LabRAM Infinity spectrometer (Jobin Yvon) equipped with a liquid nitrogen detector and a frequency-doubled Nd:YAG laser supplying the excitation line at 532 nm. The spectrometer was calibrated using the silicon line at 521 cm^{-1} . For in situ Raman analysis, the samples were placed in a temperature- and atmosphere-controlled stainless-steel cell directly adapted to the XY manual stage of the Raman microscope. The powder samples were deposited on a sintered glass disk which could be heated up to 773 K by an electrical resistor coil surrounding the sample holder. The optically polished Pyrex window the cell was 1.8-mm thick. Sample illumination and light collection proceeded with a 50-long frontal objective. The power at the sample surface was below 5 mW.

Results and Discussions

Textural characterization

Table 1 gives the textural characteristics of the investigated catalysts. Although high for such type of materials (additionally calcined at 973 K), the surface areas given in Table 1 are much smaller than those exhibited by zeolites. The increase of the W content led for all the catalysts to a

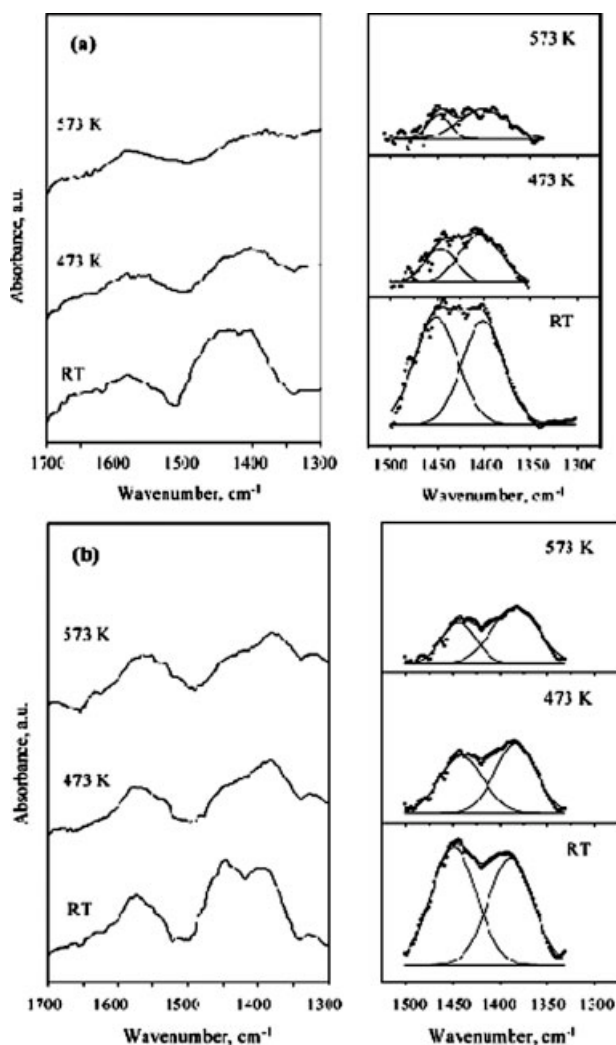


Figure 1. NH_3 -DRIFT spectra taken at different temperatures for (a) $\text{WO}_x\text{-CeO}_2\text{-10}$ and (b) $\text{WO}_x\text{-CeO}_2\text{-15}$.

decrease of the surface area. To these quite low surface areas corresponded large pores (pore diameter higher than 5 nm).

NH_3 -drift spectra

NH_3 -DRIFT spectra recorded at increasing temperatures showed bands of ammonia adsorbed both on Brønsted ($1449\text{--}1384 \text{ cm}^{-1}$) and Lewis ($1597\text{--}1530 \text{ cm}^{-1}$) acid sites. The samples calcined in air at 973 K exhibited only one band at 1430 cm^{-1} due to ammonia adsorbed on Brønsted acid sites, independent of the way the catalysts were prepared (precipitation or impregnation). These spectra clearly demonstrate that the investigated catalysts exhibit a strong acidity. In concordance, bands assigned to the adsorbed ammonia are still present at 573 K.

Figures 1a, b show the effect of the W loading on the acidity. To make this influence clearer, the spectra were reconsidered by fitting the results in the region $1350\text{--}1500 \text{ cm}^{-1}$. The comparative analysis of these spectra indicated

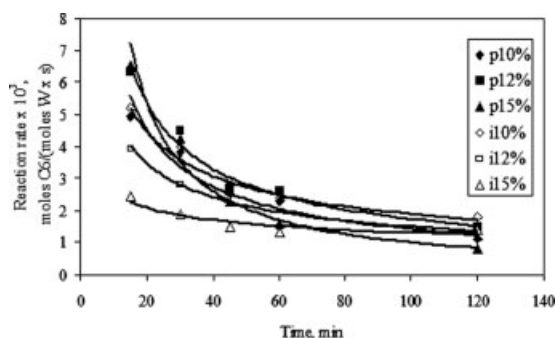


Figure 2. The time-dependence of the reaction rate, for hexane isomerization at 433 K.

that the increase of the W loading led to an increased concentration of acid sites. Also the strength of these sites appeared to be slightly enhanced by the content of W, as inferred from the comparison of the spectra at 573 K.

Catalytic activity

Time-Dependence of the Activity. Figure 2 shows the time-dependence of the reaction rate for hexane isomerization at 433 K. Both the P- and I- catalysts showed a decay in the reaction rate in the first 60 min, and then activity reached a quite stable plateau for the next hours. In the first stages, the catalysts prepared via precipitation, i.e. P-, exhibited a higher catalytic activity than those prepared by impregnation. Anyway the decay was also higher for these catalysts, and after 1 h the differences among the two series were quite small. As it was previously reported²² the influence of the W content was different for the two series of catalysts, high W content corresponding to the most active for the P-series, and less W content for the I-series.

The curves presented in Figure 2 were well fitted by an empirical equation:

$$R = m \cdot t^{-n} \quad (2)$$

which actually corresponds to the empirical Voorhies equation.^{1,6} The values of the coefficients m and n , as well of R^2 (dispersion), are given in the Table 2. The values of n confirm the higher decay of the P-catalysts at 433 K, and the fact that the increase of the W content enhances the decay of deactivation of P- catalysts, while for I-catalysts a reverse phenomenon was observed.

Table 2. The Values of m and n from Eq. 2, and of R^2 for $\text{WO}_x\text{-CeO}_2$ in the Absence of Hydrogen

Catalysts	433 K			513 K		
	m	n	R^2	m	n	R^2
P-10	39.34	0.7227	0.96	55.82	0.8542	0.96
P-12	43.87	0.7027	0.98	105.91	1.0112	0.99
P-15	123.53	1.0478	0.98	153.46	1.1046	0.95
I-10	22.08	0.5361	0.95	131.80	1.1588	0.98
I-12	16.81	0.5272	0.95	21.65	0.7247	0.99
I-15	6.42	0.3954	0.95	17.85	0.7209	0.96

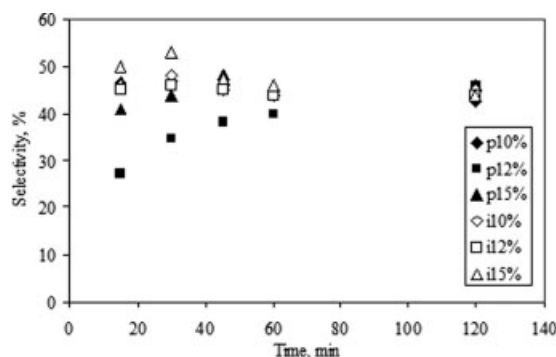


Figure 3. The variation of the selectivity to methylcyclopentane in time at 433 K.

Under the investigated conditions the main reaction products were methylcyclopentane and the monoalkylated isomers of pentane. Figure 3 shows the variation of the selectivity to methylcyclopentane in time. For the catalysts obtained via impregnation, the time variation in the selectivity to methylcyclopentane is very small irrespective of the W content. A different behavior was observed for the P-series, where the time variation of the selectivity in methylcyclopentane was found to depend on the W content and time. This was more evident for the catalyst containing 12 wt % W, where the selectivity reached a plateau after 60 min, i.e. after the time changes in the reaction rate were very small.

The increase of the temperature at 513 K led to higher reaction rates (Figure 4). The order of the activity inside the two series of the catalysts was preserved. Compared with the data recorded at 433 K the decay in the reaction rates was higher for both series of catalysts (Table 2), and the plateau was reached after a longer time, namely, after 80 min.

The increase of the temperature also caused a change in the selectivity, and under these conditions 2- and 3-methylpentanes predominate (Figure 5). For both series of catalysts the selectivity goes through a maximum after 30–50 min and then decreased reaching a plateau. For both series, the maximum value of the selectivity in methylpentanes was reached for the catalysts with the higher tungsten content. However, in time, the order in selectivity changed, following the same tendencies with those observed at 433 K.

This change in the selectivity is quite unusual since we have demonstrated in the previous paper²² that the reaction

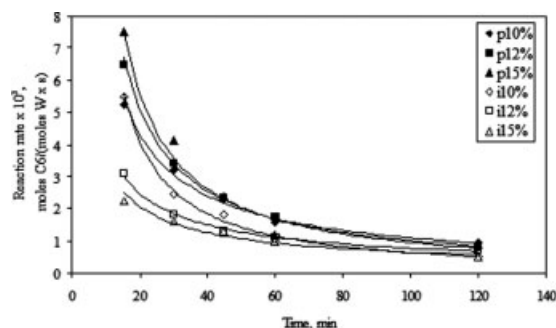


Figure 4. The time-dependence of the reaction rate for hexane isomerization at 513 K.

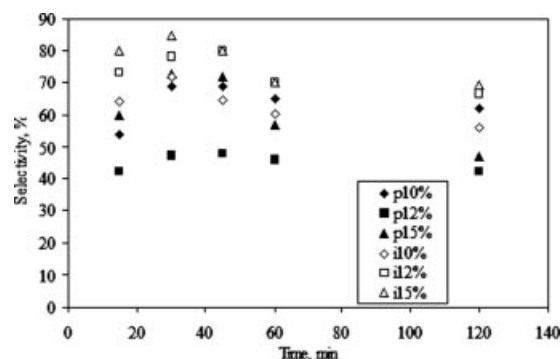


Figure 5. The variation of the selectivity to methylpentanes in time at 513 K.

to methylcyclopentane goes through hexene intermediates, and the dehydrogenation of hexane to hexenes is thermodynamically favoured by the increase of the temperature. Actually, as it will be shown further, the decrease in the selectivity to methylcyclopentane corresponded to the increase of the coke content, which is evidence that the formation of coke involves, at least in the first step, the same intermediates.

$\text{WO}_x/\text{Nb}_2\text{O}_5$ catalysts exhibited initial reaction rates higher than the corresponding ceria supported catalysts (Figure 6). However, their deactivation is slower than that found for ceria supported catalysts, and for this behavior also accounts the values of m and n given in Table 3. At 513 K, the plateau is reached after 100 min. The increase of the temperature, as for WO_x/CeO_2 , was not accomplished by changes in the activity order as a function of W loading, but only in an increased deactivation rate.

Figure 7 presents the selectivity of these catalysts at two temperatures, i.e. 433 and 513 K, after 20 min. On all these catalysts the predominant products were cyclohexane (CH) and methylcyclopentane (MCP). Benzene was found as well. The increase of the temperature led to an increase in the benzene content, concomitantly with a reduction of the selectivity in methylpentenes. The presence of CH and MCP, as well as of the benzene in the products, and the ratio MP/MCP, different on that found for WO_x/CeO_2 catalysts, sug-

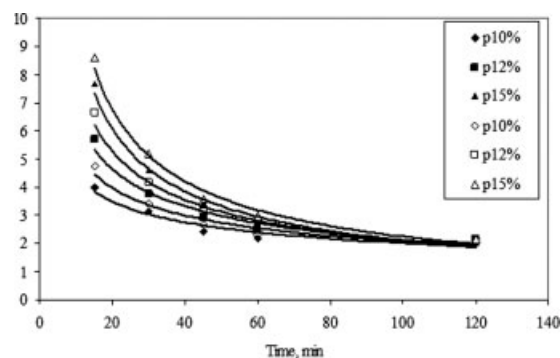


Figure 6. The time-dependence of the reaction rate for hexane isomerization on $\text{WO}_x/\text{Nb}_2\text{O}_5$ at 433 K (◆,■,▲) and 513 K (◇,□,△).

Table 3. The Values of m and n from Eq. 2, and of R^2 for Isomerization of Hexane on $\text{WO}_x/\text{Nb}_2\text{O}_5$ in the Absence of Hydrogen

Catalysts	433 K			513 K		
	m	n	R^2	m	n	R^2
P-10	9.71	0.3998	0.92	13.34	0.6841	0.98
P-12	19.74	0.4841	0.96	29.28	0.6725	0.96
P-15	43.43	0.6573	0.98	52.40	0.6986	0.98

gest a different nature of the active site for $\text{WO}_x/\text{Nb}_2\text{O}_5$. No significant change of the selectivity as a function of time has been evidenced.

Time-Dependence of the Activity in the Presence of Hydrogen. Figure 8 shows the time-dependence of the reaction rate for hexane isomerization at 433 K on WO_x/CeO_2 .

As can be seen from Figure 8 and Table 4, the presence of hydrogen led to a slight decrease of the catalytic activity, as compared with that of the same catalysts in the absence of H_2 , but under these conditions the stability of the catalysts was much increased (the n values were much smaller). Also the rate of the decay was much smaller and, as a consequence, the plateau was reached after a longer time, i.e. about 80 min.

Figure 9 shows the time evolution of the selectivity in methylpentanes at 433 K. The difference till 100% is represented by methylcyclopentane. Although a slight tendency for the decrease of the selectivity in time can be seen, it remains quite constant in time and almost independent on the amount of W and the preparation route.

The increase of the temperature at 513 K was accompanied by an increase in both the catalytic activity and the deactivation rate. However, as it can be observed from Figure 10 and Table 4, the stability of the catalysts was much increased when one compare with that at 433 K. Exception made the most active catalysts, i.e. P-15 and I-10, of which decay in the reaction rate did not, fitted the Eq. 2 with an accepted R^2 .

As in the absence of hydrogen the catalysts prepared via precipitation behaved better than the impregnated. However, the relative behavior for each series of catalysts was similar with that observed in the absence of the catalysts.

The selectivity and its variation in time at 513 K (Figure 11) were almost unchanged by comparing to that at 433 K.

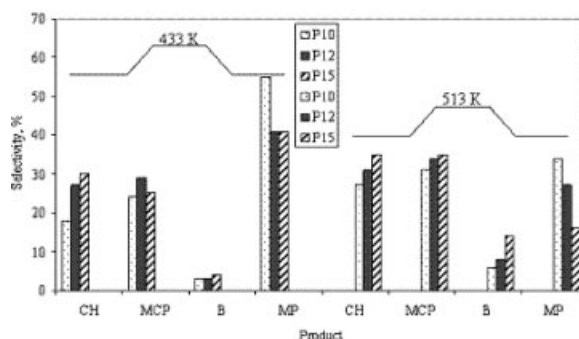


Figure 7. The selectivity in isomerization of hexane on $\text{WO}_x/\text{Nb}_2\text{O}_5$ at 433 and 513 K, after 20 min.

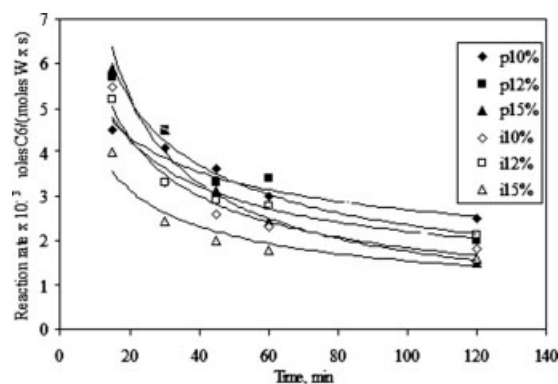


Figure 8. The time-dependence of the reaction rate for hexane isomerization at 433 K in hydrogen.

This indicates that the presence of hydrogen is indeed stabilizing the catalyst. This might be also an evidence, for the reactions carried out without hydrogen, the deposition of coke is controlling the selectivity of the reaction.

Figure 12 shows the time-dependence of the reaction rate for hexane isomerization in presence of hydrogen on $\text{WO}_x/\text{Nb}_2\text{O}_5$ at 433 and 513 K. As for WO_x/CeO_2 catalysts the activity was lowered by the presence of hydrogen. However, one also can see a large enhancement in the stability of these catalysts. The decay in the reaction rate was much smaller (Table 5).

Changes were also observed in the selectivity of these catalysts as compared with reactions carried out in the absence of hydrogen. Figure 13 shows the selectivity in isomerization of hexane in the presence of hydrogen on $\text{WO}_x/\text{Nb}_2\text{O}_5$ at 433 and 513 K, after 20 min. Under these conditions, benzene was no more detected, and the selectivity to methylpentanes increased. At 433 K these were the dominant products.

Analysis of the coke deposition

TG-DTG-HF Analysis. Figure 14 shows the TG mass loss curves for the P-12 catalyst after it was exposed to isomerization of hexane for 240 min at 433 and 513 K, respectively, in the absence and presence of hydrogen. For both catalysts coke is removed in two steps, one till about 633 K, and the other till about 973 K, which actually may correspond to two different types of coke. In the HF curve, these losses were accompanied by two exothermic peaks, the one before 633 K, showing a shoulder. This is in a perfect con-

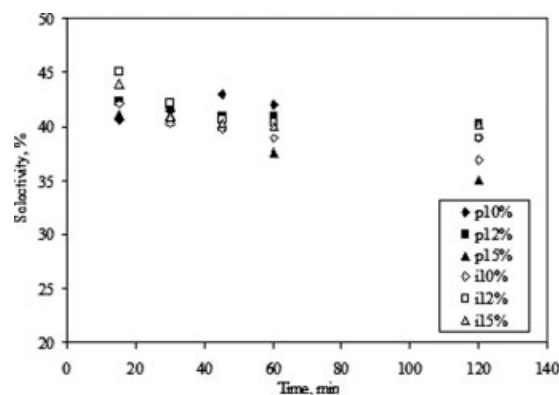


Figure 9. The variation of the selectivity to methylpentanes in time at 433 K.

cordance with TPO data reported previously for WO_x supported catalysts^{9,23} MS analysis indicated as a product of oxidation only CO_2 ($m/z = 44$).

As it results from this figure the total amount of coke released from the two samples is different. For the catalysts reacted at 433 K, the mass loss corresponded to 3.78 wt % of the mass of the catalyst, while for catalysts reacted at 513 K, the loss corresponded to 5.18 wt % of the mass of the catalyst. Very interestingly is the way in which the percent of the coke removed by heating was correlated with the values of n from Eq. 2. This dependency is given in Figure 15 and presents a very good correlation. The values of R^2 were higher than 0.93.

Figure 16 shows the TG mass loss for the same P-12 catalyst reacted in the presence of hydrogen. The mass loss was at both temperatures almost five times smaller than that found for the catalyst tested in the absence of hydrogen. In contradiction with the curves presented in Figure 14, the mass lost for the catalyst tested in the presence of hydrogen, presents a single loss, which ends before 673 K. This might suggest that under these conditions a single type of coke was formed. However, in the HF curve, this loss was accompanied by two exothermic peaks, which might indicate the formation of two different species. Nishiguchi et al.²³ also

Table 4. The Values of m and n from Eq. 2, and of R^2 for $\text{WO}_x\text{-CeO}_2$ in the Presence of Hydrogen

Catalysts	433 K			513 K		
	m	n	R^2	m	n	R^2
P-10	10.65	0.2981	0.95	12.46	0.4048	0.97
P-12	22.92	0.4952	0.96	24.05	0.5025	0.98
P-15	40.59	0.6820	0.98		No fitted	
I-10	21.32	0.5326	0.96		No fitted	
I-12	14.74	0.4132	0.95	16.01	0.4903	0.97
I-15	11.79	0.4422	0.91	13.26	0.5379	0.95

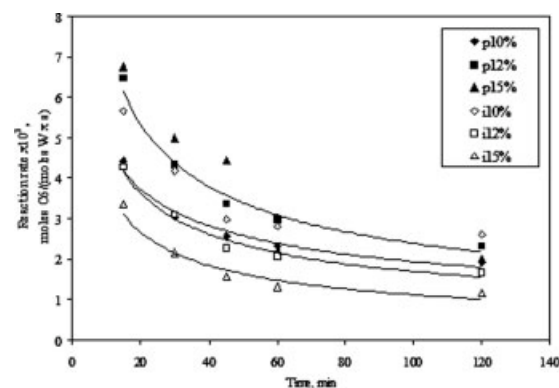


Figure 10. The time-dependence of the reaction rate for hexane isomerization at 513 K in hydrogen.

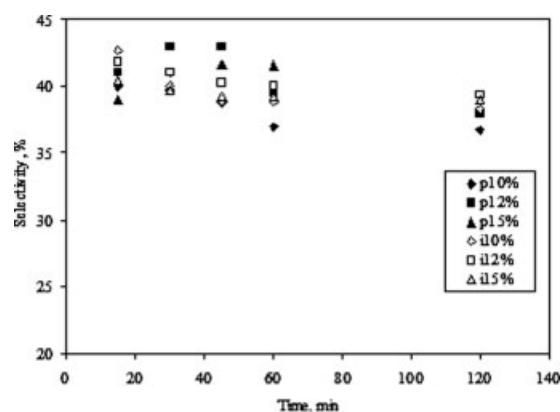


Figure 11. The variation of the selectivity to methylpentanes in time at 513 K.

reported for a WO_x/ZrO_2 catalyst from a TPO investigation the presence of two species before 573 K. According to Matsushita et al.⁷ the two fractions of coke can be classified as a reactive soft coke, which can be removed more easily, and as a refractory surface coke, which is strongly adsorbed at the catalyst support. The last category corresponds actually to the coke found for the catalyst tested without hydrogen at temperatures higher than 673 K.

The decrease of the coke deposition with the increase of the hydrogen pressure is in a good agreement with data reported previously.²⁴

As for the catalysts tested in the absence of hydrogen, a very good correlation was obtained between the percent of the mass loss and the values of n determined from Eq. 2 (Figure 15). The slope of this dependency is lower than that found for the catalysts tested in the absence of hydrogen, which may again be related to the different rates of deactivation.

TG analysis of the $\text{WO}_x\text{-Nb}_2\text{O}_5$, in a good accordance with the catalytic time-evolution results, indicated a smaller amount of coke, thus corresponding evidently to a better stability. Figure 17 gives the TG mass loss during heating in 10% O_2/He atmosphere of $\text{WO}_x\text{-Nb}_2\text{O}_5$ P-12 catalyst reacted in the presence of H_2 . As for the $\text{WO}_x\text{-CeO}_2$ catalysts reacted

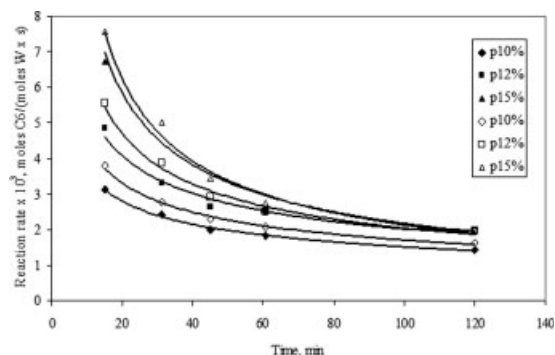


Figure 12. The time-dependence of the reaction rate for hexane isomerization in presence of hydrogen on $\text{WO}_x/\text{Nb}_2\text{O}_5$ at 433 K (◆,■,▲) and 513 K (◇,□,△).

Table 5. The Values of m and n from Eq. 2, and of R^2 for Isomerization of Hexane on $\text{WO}_x/\text{Nb}_2\text{O}_5$ Catalysts in Hydrogen

Catalysts	433 K			513 K		
	m	n	R^2	m	n	R^2
P-10	8.73	0.3798	0.99	11.38	0.4123	0.99
P-12	14.97	0.4334	0.97	21.98	0.5156	0.98
P-15	36.74	0.6137	0.97	45.93	0.6666	0.98

under similar conditions, the coke is removed before 673 K. However, as mentioned before the amount of coke was much smaller (0.41 wt %). For the catalysts reacted in the absence of hydrogen two types of coke have been also evidenced, one removed before 673 K, and the other removed before 873 K (curves not shown).

Again, a very good correlation between the percent of the coke removed by heating and the values of n from Eq. 2 was found. This dependency is given in Figure 18. The values of R^2 were higher than 0.93. Like for $\text{WO}_x\text{-CeO}_2$ catalysts the slope resulted for the catalysts reacted in the absence of hydrogen was higher, in agreement with the higher deactivation rate of these catalysts.

In-Situ Raman Measurements. The Raman spectrum of 15% WO_x/CeO_2 catalyst (Figure 19a) exhibits an intense line at 462 cm^{-1} that is characteristic of crystalline CeO_2 and also two sharp lines at 924 and 942 cm^{-1} assigned to well crystallized $\text{Ce}_2(\text{WO}_4)_3$.²² Moreover, we can exclude the formation of WO_3 whose major Raman line is expected at 806 cm^{-1} . During the pre-treatment under hydrogen and also during the reaction mixture under hexane/ H_2 , no change occurred in the region of the polytungstate species lines (Figure 19b). However, for the in-situ spectra collected during the reaction of hexane in hydrogen or directly (Figures 19b, c) we can notice the appearance and further increase of two broad and intense lines located at 1375 and 1582 cm^{-1} . Based on literature data of relevant reference compounds, these two Raman lines can be assigned to the formation of polyaromatic hydrocarbons or coke.²⁵ The existence of the two bands is in line with the assumption made from thermal investigation of the tested catalysts about the generation of two different types of coke.

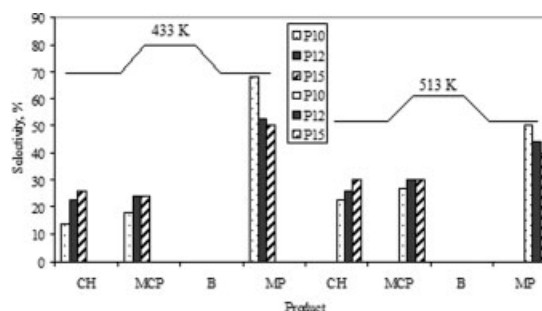


Figure 13. The selectivity in isomerization of hexane in the presence of hydrogen on $\text{WO}_x/\text{Nb}_2\text{O}_5$ at 433 K and 513 K.

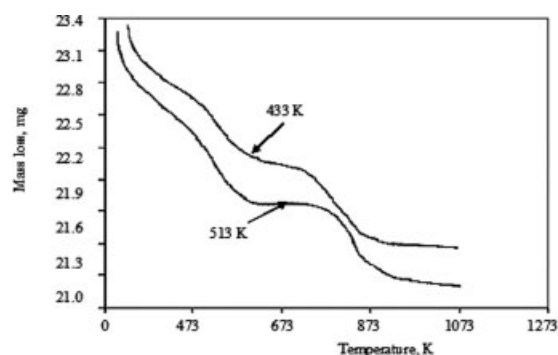


Figure 14. TG mass loss during heating in 10% O₂/He atmosphere of P-12 catalyst reacted in the absence of hydrogen.

The Raman spectrum of 15% WO_x/Nb₂O₅ catalyst at ambient temperature exhibits several broad lines whose most intense are located at 664 and 847 cm⁻¹ (Figure 20). This Raman spectrum can be considered as characteristic of bulk Nb₂O₅ support.²⁶ Unfortunately, the Raman line due to the terminal W=O bond of the surface tungstate species, which is expected in the 900–1000 cm⁻¹ spectral region, is not observed.²⁷

Under activation in hydrogen no changes occurred in these spectra. However, during the reaction mixture under hexane/H₂ or under hexane one can also observe the formation of coke like on the 15% WO_x/CeO₂ catalysts. The formation of coke was less rapid for niobia based catalysts.

Complementary informations were collected from the FTIR analysis of the tested catalysts (spectra not shown). For all the investigated catalysts, irrespective of the temperature they have been exposed to the reaction, or of the W content or the preparation procedure, absorption bands in the region 1600–1500 cm⁻¹, assigned to C=C double bonds have been evidenced.

Post Solvent Extraction. Post extraction of coked catalysts, e.g. Soxhlet-extraction with THF, toluene, CH₂Cl₂ or CHCl₃ and analysis of the resulted solution by MS indicated the presence of a large number of hydrocarbon compounds with number of carbon atoms smaller the 10. This is actually corresponding to the soft coke. Further TG analysis of the extracted catalysts indicated no mass loss before 513 K, thus confirming this supposition. However, for the catalysts tested

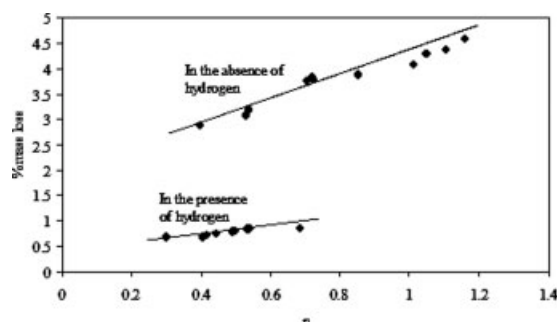


Figure 15. The correlation of the percent of the mass loss with *n* for the WO_x-CeO₂ catalysts tested in the presence of hydrogen.

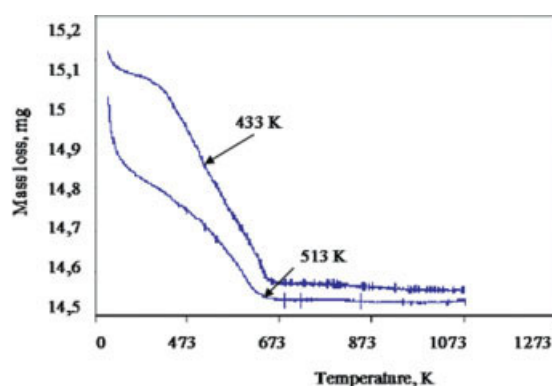


Figure 16. TG mass loss during heating in 10% O₂/He atmosphere of P-12 catalyst tested in the presence of H₂.

[Color figure can be viewed in the online issue, which is available at www.interscience.wiley.com.]

in the absence of hydrogen this peak was still persistent, confirming the fact that this coke is not soluble in the usual molecular solvents.

General assessments

All the investigated catalysts showed a time deactivation, irrespective of the preparation method (precipitation or impregnation), tungsten loading, or support nature. However, these data evidenced a clear difference between the catalysts with different W loading, between the catalysts supported on CeO₂ or Nb₂O₅, and between the catalysts tested in the absence or in the presence of hydrogen. As a general behavior, the more active catalysts deactivated more quickly, and this was always the case of P-series as compared to the I-series. As well, the catalyst with 15 wt % W for the P series, and that with 10 wt % W for the I-series deactivated more quickly than the other catalysts from that series.

Among these factors, three seem to exhibit a stronger effect. As expected the increase of the temperature led to higher amounts of coke, and especially to the formation of what is named refractory surface coke. On the contrary, the

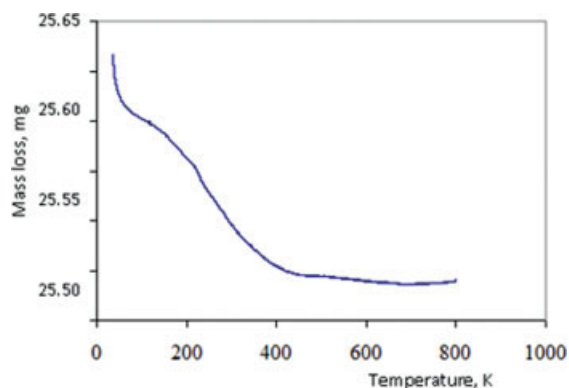


Figure 17. TG mass loss during heating in 10% O₂/He atmosphere of WO_x/Nb₂O₅ P-12 catalyst reacted in the presence of H₂.

[Color figure can be viewed in the online issue, which is available at www.interscience.wiley.com.]

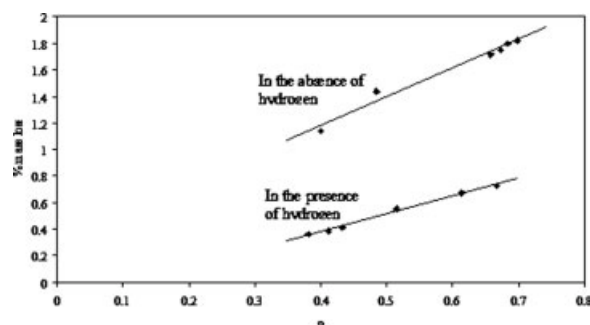


Figure 18. The correlation of the percent of the mass loss with n for the $\text{WO}_x/\text{Nb}_2\text{O}_5$ catalysts tested in the presence of hydrogen.

presence of hydrogen inhibits the catalytic activity, but also the formation of coke. Its presence mostly determines the formation of the soft coke. The third important parameter controlling the deactivation seems to be the nature of the support. Cerium oxide is a used support mostly because it exhibits well known oxidative properties. We have demonstrated that in combination with tungsten it leads to active catalysts in isomerization of hexane.²² The presence of CeO_2 enhances the oxidative properties of the support, favoring the activation of alkenes via a hydrogen subtraction. These hexenes can isomerize on the catalysts acid sites, or they can follow the mechanism of the reaction described by the left part in the Scheme 1. According to this they may undergo a transformation to methylcyclopentane and then to the soft coke, and at higher temperatures, the soft coke is transformed via a hydrogen transfer or a polymerization into a refractory surface coke.

For the catalysts containing niobia such a mechanism is less probable, since niobia exhibits a smaller oxidative behavior, and stronger acid characteristics. Therefore, for these catalysts, is more probable an ionic-radicalic mechanism as that demonstrated previously for sulfated zirconia.²⁸ According to this mechanism in the first step occurs only

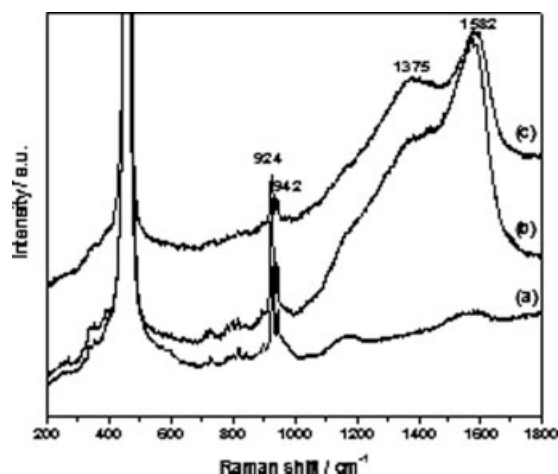


Figure 19. In situ Raman spectra of 15% WO_x/CeO_2 . (a) Under air at 298 K, (b) under hexane/ H_2 at 513 K for 2h30, and (c) under hexane at 513 K for 2h30.

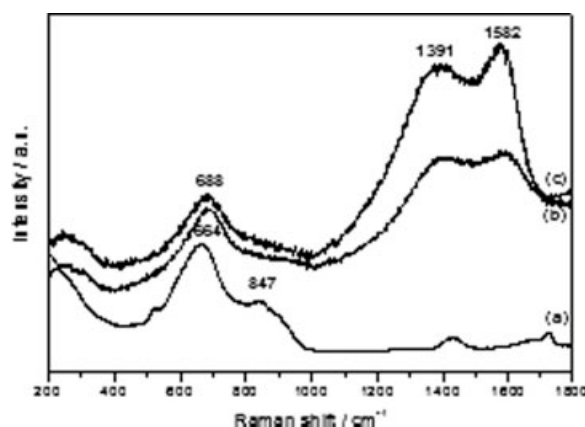


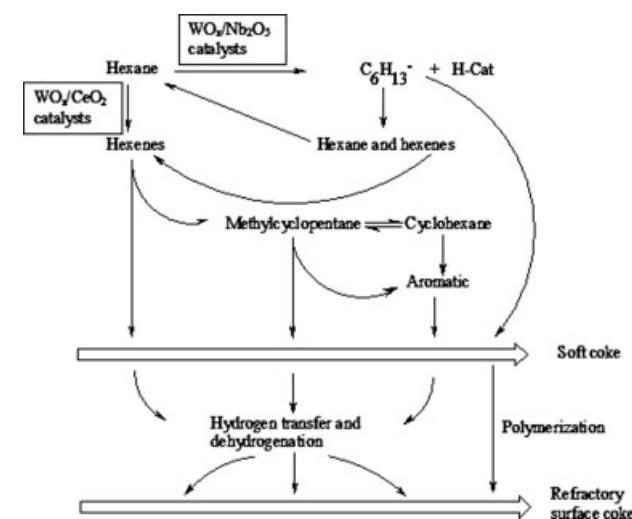
Figure 20. In situ Raman spectra of 15% $\text{WO}_x/\text{Nb}_2\text{O}_5$. (a) Under air at 298 K, (b) under hexane/ H_2 at 513 K for 1h30, and (c) under hexane at 513 K for 1h30.

one hydrogen subtraction with the formation of the radical, which then in a second step could disproportionate: leading to hexenes which can give isomerization or cyclization to CH or MCP, or could polymerize giving catalyst deactivation (left part in Scheme 1). Another source of the catalyst deactivation in this case is the polymerization of the radicalic species itself.

The presence of hydrogen limits the deactivation till a certain extent because it limits the further dehydrogenation of the intermediates to aromatics, and their polymerization to polyaromatics. TG analysis of the samples reacted in the absence and the presence of hydrogen is a good probe for this. The samples reacted in hydrogen contained only soft coke. In situ Raman and FTIR experiments provided additional information in this sense.

Conclusions

Deactivation of tungsten based catalysts in isomerization of hexane was found to depend on several factors like the



Scheme 1. The mechanism of coke formation on the catalysts investigated.

preparation method (precipitation or impregnation), tungsten loading, or support nature. The catalysts with high loading of W and those prepared by precipitation deactivated more quickly than the others. Also, the catalysts deposited on niobia deactivated more rapidly than those deposited on ceria. The presence of hydrogen diminished the deactivation rate and favored mostly the formation of soft coke.

The deactivation rate was very well fitted by an empirical Vorhies equation: $r = m \cdot t^{-n}$. The values of n from this equation correlated very well with the mass loss determined from TG analysis. In situ Raman and FTIR experiments provided additional information about the formation of coke and its nature.

Literature Cited

1. Rostrup-Nielsen JR. Industrial relevance of coking. *Catal Today*. 1997;37:225–232.
2. Marin GB, Beeckman JW, Froment GF. Rigorous kinetic models for catalyst deactivation by coke deposition: application to butene dehydrogenation. *J Catal*. 1986;97:416–426.
3. Beeckman JW, Froment GF. Catalyst deactivation by active site coverage and pore blockage. *Ind Eng Chem Fundam*. 1979;18:245–256.
4. Beeckman JW, Froment GF. Deactivation of catalysts by coke formation in the presence of internal diffusional limitation. *Ind Eng Chem Fundam*. 1982;27:243–250.
5. Beeckman JW, Froment GF. Catalyst deactivation by site coverage and pore blockage. *Chem Eng Sci*. 1980;35:805–809.
6. Naccache C. *Deactivation of Acid Catalysts in Deactivation and Poisoning of Catalysts*. New York: Marcel Dekker, 1985:185–203.
7. Matsushita K, Hauserb A, Marafic A, Koidea R, Stanislaus A. Initial coke deposition on hydrotreating catalysts. Part 1. Changes in coke properties as a function of time on stream. *Fuel*. 2004;83:1031–1038.
8. Quennl CA, Fung SC. Coke characterization by temperature programmed techniques. *Catal Today*. 1997;37:277–283.
9. Benitez VM, Querini CA, Figoli NS. Characterization of WO_x/Al₂O₃ and MoO_x/Al₂O₃ catalysts and their activity and deactivation during skeletal isomerization of 1-butene. *Appl Catal A*. 2003;252:427–436.
10. Snape CE, McGhee BJ, Martin SC, Andresen JM. Structural characterization of catalytic coke by solid-state ¹³C-NMR spectroscopy. *Catal Today*. 1997;37:285–293.
11. Martin N, Viniegra M, Lima E, Espinosa G. Coke characterization on Pt/Al₂O₃- β -zeolite reforming catalysts. *Ind Eng Chem Res*. 2004;43:1206–1210.
12. Wood J, Gladden LF. Effect of coke deposition upon pore structure and self-diffusion in deactivated industrial hydroprocessing catalysts. *Appl Catal A*. 2003;249:241–253.
13. Martens JA, Souverijns W, Verrelst W, Parton R, Gromont GF, Jacobs PA. Selective isomerization of hydrocarbon chains on external surfaces of zeolite crystals. *Angew Chem*. 1995;34:2528–2530.
14. Iglesia E, Barton DG, Soled SL, Misco S, Baumgartner JE, Gates WE, Fuentes GA, Meitzner GD. Selective isomerization of alkanes on supported tungsten oxide acids. *Stud Surf Sci Catal*. 1996;101:533–542.
15. Makoto H, Kazushi A. Synthesis of solid superacid catalyst with acid strength of $H_0 \leq -16.04$. *J Chem Soc Chem Commun*. 1980;851–852.
16. Părvulescu VI, Coman S, Părvulescu V, Poncelet G. TG and DTA investigation of ZrO₂.SO₄-catalysts exposed to hexane, methylcyclopentane, and cyclohexane. *Catal Lett*. 1998;52:231–238.
17. Părvulescu V, Coman S, Părvulescu VI, Grange P, Poncelet G. Reaction of hexane, cyclohexane, and methylcyclopentane over gallium-, indium-, and thallium-promoted sulfated zirconia catalysts. *J Catal*. 1998;180:66–84.
18. Keogh RA, Sparks DE, Davis BH. Deactivation of Pt/ZrO₂/SO₄ catalyst. *Stud Surf Sci Catal*. 1994;88:647–654.
19. Garin F, Andriamasinoro D, Abdulsamad A, Sommer J. Conversion of butane over the solid superacid ZrO₂/SO₄²⁻ in the presence of hydrogen. *J Catal*. 1991;131:199–203.
20. Vaudagna SR, Comelli RA, Canavese SA, Figoli NS. SO₄/ZrO₂ and Pt/SO₄/ZrO₂: activity and stability during *n*-hexane isomerization. *J Catal*. 1997;169:389–393.
21. Zhang Z, Lerner B, Lei GD, Sachtler WMH. Hydrocarbon-induced agglomeration of Pd particles in Pd/HZSM-5. *J Catal*. 1993;140:481–496.
22. Mamede AS, Payen E, Grange P, Poncelet G, Ion A, Alifanti M, Părvulescu VI. Characterization of WO_x/CeO₂ catalysts and their reactivity in isomerization of hexane. *J Catal*. 2004;223:1–12.
23. Nishiguchi T, Oka K, Matsumoto T, Kanai H, Utani K, Imamura S. Durability of WO₃/ZrO₂-CuO/CeO₂ catalysts for steam reforming of dimethyl ether. *Appl Catal A*. 2006;301:66–74.
24. Richardson SM, Nagaishi H, Gray MR. Initial coke deposition on a NiMo/ γ -Al₂O₃ bitumen hydroprocessing catalyst. *Ind Eng Chem Res*. 1996;35:3940–3950.
25. Chua YT, Stair PC. An ultraviolet Raman spectroscopic study of coke formation in methanol to hydrocarbons conversion over zeolite H-MFI. *J Catal*. 2003;213:39–46.
26. Gao X, Wachs IE, Wong MS, Ying JY. Structural and reactivity properties of Nb-MCM-41: comparison with that of highly dispersed Nb₂O₅/SiO₂ catalysts. *J Catal*. 2001;203:18–24.
27. Kim DS, Ostromecki M, Wachs, IE. Surface structures of supported tungsten oxide catalysts under dehydrated conditions. *J Mol Catal A*. 1996;106:93–102.
28. Coman S, Parvulescu V, Grange P, Parvulescu VI. Transformation of C₆ hydrocarbons over sulfated zirconia catalysts. *Appl Catal A*. 1999;176:45–62.

Manuscript received Nov. 23, 2007, and revision received Jan. 21, 2008.